Vol 18 No 3, March 2009
1674-1056/2009/18(03)/1242-06
Chinese Physics B
© 2009 Chin. Phys. Soc.
and IOP Publishing Ltd

A novel micro-accelerometer with adjustable sensitivity based on resonant tunnelling diodes*

Xiong Ji-Jun(熊继军)[a)†], Mao Hai-Yang(毛海央)[b)],
Zhang Wen-Dong(张文栋)[a)], and Wang Kai-Qun(王楷群)[a)]

[a)] *Key Laboratory of Instrumentation Science and Dynamic Measurement of the Ministry Education, North University of China, Taiyuan* 030051, *China*

[b)] *Institute of Microelectronics, Peking University, Beijing* 100871, *China*

(Received 15 June 2008; revised manuscript received 8 August 2008)

Resonant tunnelling diodes (RTDs) have negative differential resistance effect, and the current–voltage characteristics change as a function of external stress, which is regarded as meso-piezoresistance effect of RTDs. In this paper, a novel micro-accelerometer based on AlAs/GaAs/$In_{0.1}Ga_{0.9}As$/GaAs/AlAs RTDs is designed and fabricated to be a four-beam-mass structure, and an RTD-Wheatstone bridge measurement system is established to test the basic properties of this novel accelerometer. According to the experimental results, the sensitivity of the RTD based micro-accelerometer is adjustable within a range of 3 orders when the bias voltage of the sensor changes. The largest sensitivity of this RTD based micro-accelerometer is 560.2025 mV/g which is about 10 times larger than that of silicon based micro piezoresistive accelerometer, while the smallest one is 1.49135 mV/g.

Keywords: micro-accelerometer, piezoresistance effect, resonant tunnelling diode (RTD), sensitivity
PACC: 7360L, 7980

1. Introduction

Since the first observation of negative differential resistance (NDR) in the double barrier quantum well structure,[1] researches on resonant tunnelling diodes (RTDs) have been done for two decades. RTDs, with features such as high speed, high frequency, low voltage and power, have been extensively adopted in digital-logical circuit, analogy circuit, signal process and digital–analogy converting circuit as well as micro wave.[2−5] Oscillations up to 712 GHz have been reported and several applications of RTDs for multi-valued logic have been proposed.[6,7] Recently, researchers found that the current–voltage characteristics of RTDs are very sensitive to mechanical signals,[8−11] especially in the NDR region, this is regarded as a meso-piezoresistance effect of RTDs.[12−14] In the aspect of quantum principle, this effect can be explained as follows: when a mechanical signal is applied to RTD, a stress distribution will be generated in the quantum well structure; such a stress distribution will originate an inner electrical field in the quantum well; the existence of the inner electrical field will result in changes of the quantum energy level; the change of quantum energy level will finally cause a variation in resonant tunnelling current. In short, the current–voltage characteristic of RTD will be changed when the applied mechanical load changes. At a certain biased resonant tunnelling voltage, the relation between mechanical load and tunnelling current can be equivalent to that between mechanical load and resistance variation.[15,16]

Wang Jian discussed the pressure effects on AlAs/InGaAs/GaAs RTDs, in Ref.[17], he contributed the shift of current–voltage characteristics of [001]-oriented AlAs/InGaAs/GaAs RTDs to uniaxial external stress applied parallel to the [110] and the $[1\bar{1}0]$ orientations. Fobelets *et al* designed an RTD based micro-pressure sensor, using the selective etch of GaAs with AlAs as an etch stop layer.[13] Mutamba *et al* reported an RTD based pressure sensor similar with that of Fobelets'. In their sensor, the relaxation frequency of RTDs as a function of pressure was used to obtain the value of the pressure. They discussed the frequency output characteristics of the sensor in detail, the sensitivity of this sensor was measured to

*Project supported in part by the National Natural Science Foundation of China (Grant No 50775209), the Fork Ying Tung Education Foundation (Grant No 101052) and Program for Excellent Talents by Ministry of Education of China.
†Corresponding author. E-mail: xiongjijun@nuc.edu.cn

be 0.8 kHz/MPa.[18,19] Researchers also found that the RTD based piezoresistance effect has many advantages over that based on silicon,[20,21] the influence of temperature on RTD based piezoresistance effect is smaller, what is more, the piezoresistive sensitivity is much higher. The last but not least, the resistance changing ratio of RTD is adjustable when the bias voltage of RTD is changed. Therefore, the sensitivity of the accelerometer is adjustable by changing the bias voltage.

In this paper, a GaAs/AlAs/InGaAs double barrier RTD based novel micro-accelerometer with adjustable sensitivity is designed and fabricated, and an RTD-Wheatstone bridge measurement system is established to detect the performance of the accelerometer. According to the experimental results, the sensitivity of this RTD based micro-accelerometer is much higher than that of silicon based sensor with the same structure and the same dimensions. What is more, when change the bias voltage of the RTD, the sensitivity can be adjustable within a range of three orders.

2. Structure design and fabrications

The micro-accelerometer studied in this paper utilizes a four-beam-mass structure. To utilize the stress caused by acceleration loading most effectively, four RTDs are grown at the base of each beam, as shown in Fig.1. The resonant tunnelling structure, which is the stress sensing component in an RTD structure, is very small in dimension and can be regarded as a point, therefore, it experiences the largest stress and strain of the beam-mass structure.

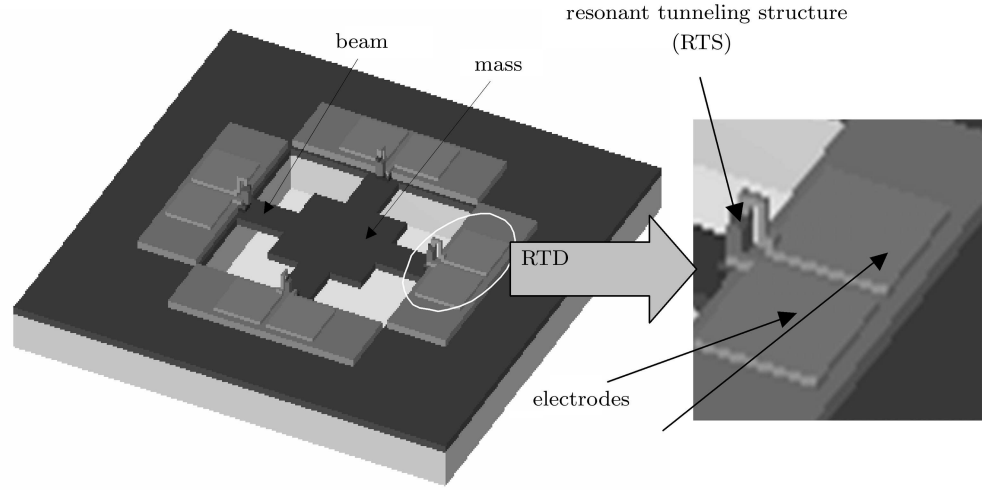


Fig.1. Beam-mass structure and RTD distributions. The RTDs are grown on a [001]-oriented undoped (semi-insulating) GaAs substrate. Each RTD consists of an RTS and two electrodes.

By using the molecular beam epitaxy technique, RTD material structures were successfully grown on the GaAs substrate. The most important part of an RTD is the AlAs/GaAs/$In_{0.1}Ga_{0.9}As$/GaAs/AlAs double barrier single quantum well structure. Later, an etching step was adopted to release the RTD structures. The structure and dimensions of RTD material is shown in Fig.2, from which we can see that two 5 nm undoped $In_{0.1}Ga_{0.9}As$ layers were inserted into the insulating layers of the collector and emitter region. The purpose for doing so is to form a pre-well between the emitter region and the barrier region. In the pre-well there exist discrete energy levels, thus this structure transfers the resonant tunnelling between the emitter region and well to that between the pre-well and well, which will result in a lower peak-voltage, a higher peak to valley current ratio (PVCR), a smaller area of emitter and a reduced latent capacitance. Furthermore, to reduce the parasitic capacitance and eliminate the marginal problem, a lift-off (double-air-bridging) technique was adopted to connect the electrodes with mesa located on the buffer layer.

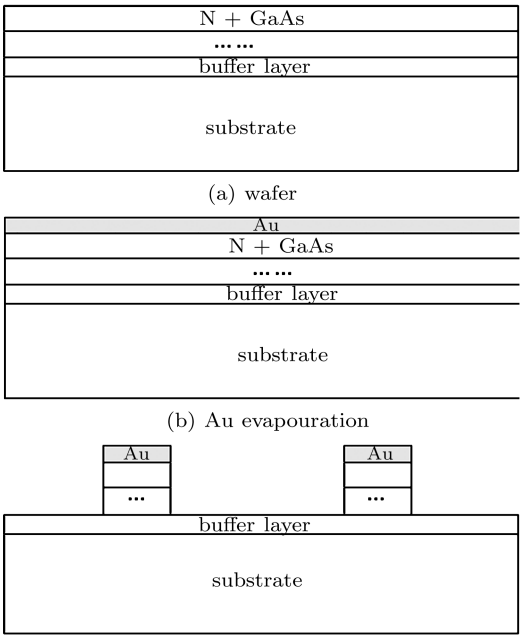
Based on the GaAs bulk micromachining process, the beam-mass structure was fabricated. Firstly, mesas are defined by photolithography on the epitaxial surface using reactive ion etching. A Si_3N_4 membrane is deposited and patterned to isolate the emitter and collector electrodes. A thick polyimide layer is used as sacrificial layer. The top of the structure is totally covered by polyimide except for the contact area on

the diode mesa and the Si_3N_4 membrane. AuGeNi/Au ohmic contacts are used and alloyed at 380°C. Then the double air-bridge electrode is processed by eroding the polyimide layer (sacrificial layer).

N^+-GaAs	$3 \times 10^{18}\,cm^{-3}$	500 nm
N^+-GaAs	$10^{17}\,cm^{-3}$	10 nm
GaAs	undouped (UD)	5 nm
$In_{0.1}Ga_{0.9}As$	UD	5 nm
GaAs	UD	0.5 nm
AlAs	UD	1.7 nm
GaAs	UD	0.5 nm
$In_{0.1}Ga_{0.9}As$	UD	4 nm
GaAs	UD	0.5 nm
AlAs	UD	1.7 nm
GaAs	UD	0.5 nm
$In_{0.1}Ga_{0.9}As$	UD	5 nm
GaAs	UD	5 nm
N^+-GaAs	$10^{17}\,cm^{-3}$	10 nm
N^+-GaAs	$3 \times 10^{18}\,cm^{-3}$	1000 nm
SI-GaAs substrate		

Fig.2. Material and dimensions of RTD. The most important part of an RTD is the AlAs/GaAs/$In_{0.1}Ga_{0.9}As$/GaAs/AlAs double barrier single quantum well structure, where two 4 nm undoped $In_{0.1}Ga_{0.9}As$ layers are inserted into the insulating layers of the collector and emitter region.

Figure 3 shows the fabrication process.



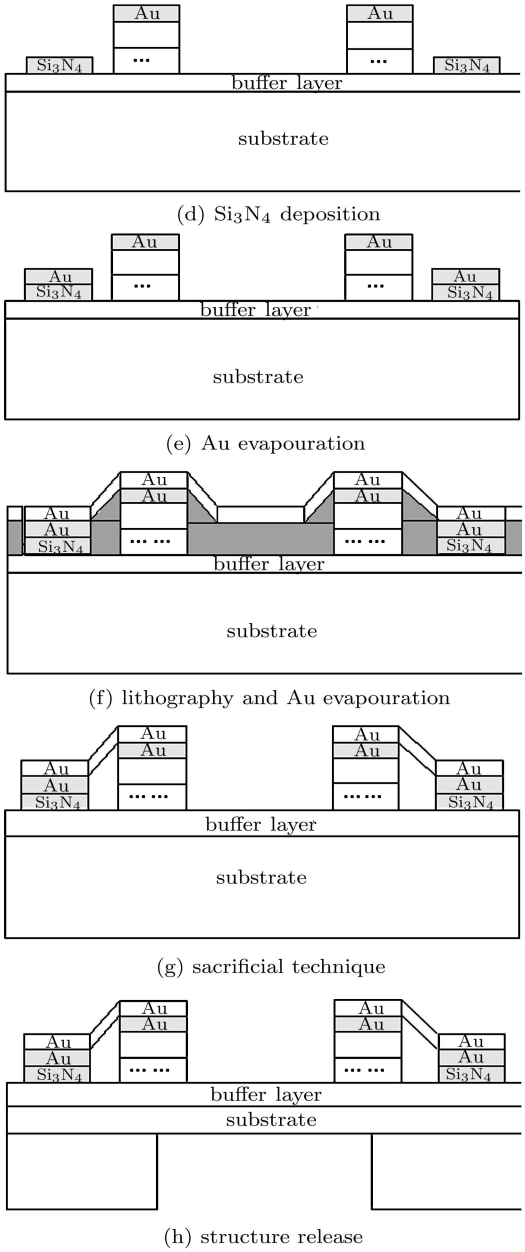


Fig.3. Fabrication process of the RTD based micro-accelerometer.

Figure 4 shows a scanning electron microscope (SEM) image of the double-air-bridging structure in RTD.

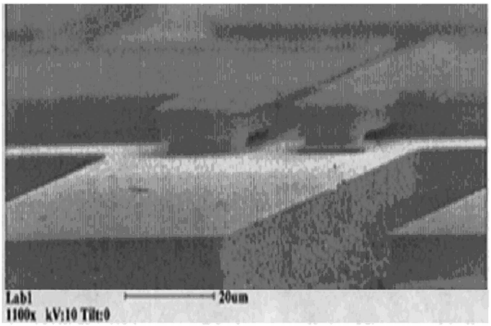


Fig.4. SEM image of an RTD with double-air-bridging.

Figure 5 shows a SEM image of the RTD based micro-accelerometer.

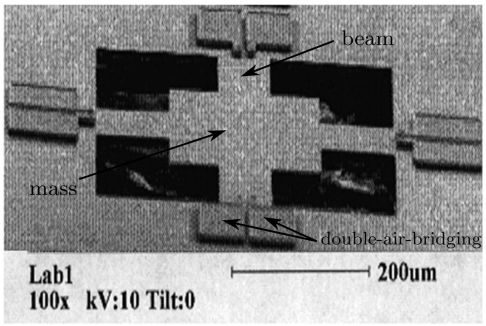


Fig.5. SEM image of a micro-accelerometer.

3. Measurement description

To detect the performance of the RTD based micro-accelerometer, an RTD-Wheatstone bridge based experiment system is established. The experimental system consists of a vibration calibrator and its computer controlling system, a bridge testing circuit, an oscillograph and a signal recorder. In the experiment, the micro-accelerometer is stuck firmly on the platform of the calibrator, the parameters of the external acceleration are set by the computer controlling system, the testing circuit is used to put out and deal with the voltage signals. Meanwhile, the voltage waves are shown by the oscillograph and recorded by the signal recorder. Taking one of the RTDs in the micro -structure as a changing resistor, connecting it with two fixed resistors (namely R_1) and an adjustable resistor (R_2), we construct an RTD-Wheatstone bridge, as shown in Fig.6. When there is an external acceleration loading on the structure, the resistance of RTD is changed, leading to a variation of the output voltage. Taking the relation between the output voltage and the acceleration as a foundation, the acceleration measurement is realized.

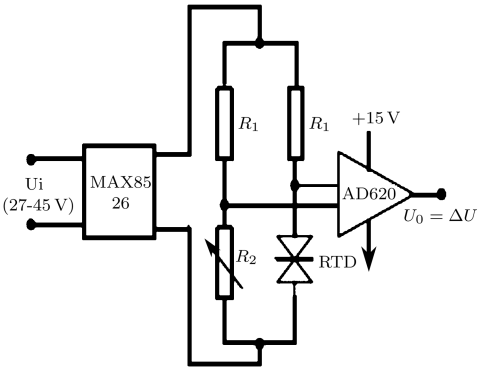


Fig.6. Schematic of the RTD-Wheatstone bridge circuit. MAX8526 is used as regulator to provide stable voltage for the circuit, AD620 is an operation amplifier used to amplify the output signal of the bridge circuit.

Suppose the output voltage of the circuit is V, the magnification factor of the circuit is G, there is

$$V = \left(\frac{R_x}{R_1 + R_x} V_0 - \frac{R_2}{R_1 + R_2} V_0 \right) G. \qquad (1)$$

With an initial condition of $R_2 = R_x$, there is $V = 0$. If there is an acceleration load, a ΔR_x in the resistance of RTD occurs, thus the output voltage is

$$V = \left(\frac{R_x + \Delta R_x}{R_1 + R_x + \Delta R_x} V_0 - \frac{R_x}{R_1 + R_x} V_0 \right) G. \qquad (2)$$

Because the value of the serial resistor R_1 affects the descending slope of RTD greatly, thus, R_1 is fixed to be 1Ω .Therefore, when the output voltage corresponding to the acceleration is known, the acceleration sensitivity can be obtained.

At the beginning of the experiment, the current–voltage characteristic of RTD without any external acceleration is detected, as shown in Fig.7, in which the dashed lines illustrate the NDR region of RTD. According to such a characteristic, the resistances of RTD at different bias voltage are obtained, as shown in Fig.8. In Fig.8, we find that at the bias voltages of 0.618 V, 0.623 V and 0.655 V, the resistances of RTD are 51.933Ω, 55.643Ω and 172.876Ω, respectively. When there are acceleration loads, the resistances of RTD at these bias voltages will change, which will lead to different output voltages.

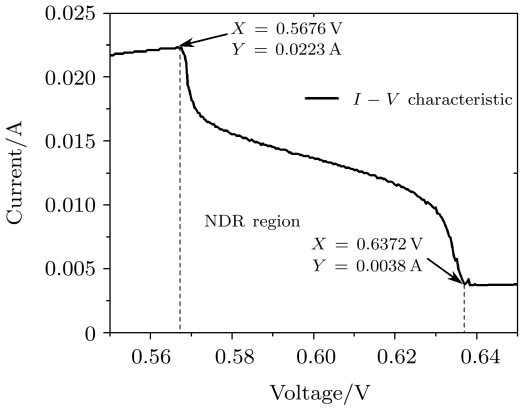


Fig.7. Current–voltage curve at normal stress status.

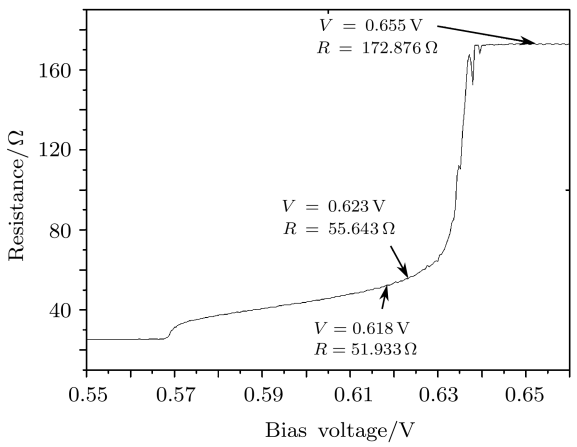


Fig.8. Resistance versus voltage at normal stress status.

Firstly, the bias voltage is adjusted within the NDR region of RTD ($V_0 \approx 0.623\,\mathrm{V}$), change R_2 to make the bridge in the state of balance, the frequency of the sinusoidal acceleration from the vibration calibrator is fixed to be 320 Hz, and the output voltage signals at different acceleration amplitude are detected, the obtained voltage–acceleration curve is shown in Fig.9. According to Fig.9, we obtain 90.51 mV/g for the RTD-Wheatstone bridge based acceleration sensitivity at $V_0 \approx 0.623\,\mathrm{V}$.

The calculated nonlinear value is 5.967% in Fig.9. The reason why the nonlinear value is a little big is because RTDs are put at the rim of the micro-accelerometer. Based on the ANSYS simulation results of stress, the rim of the micro-accelerometer is nonlinear region which will lead to big nonlinear value.

Then the bias voltage is set to be $V_0 = 0.748\,\mathrm{V}$, which is beyond the NDR region of RTD. The voltage-acceleration curve at such a state is obtained, as shown in Fig.10, according to which the acceleration sensitivity is 2.39 mV/g. Similarly, when changing the bias voltage, the acceleration detecting sensitivities at different bias voltage are obtained, as shown in Fig.11.

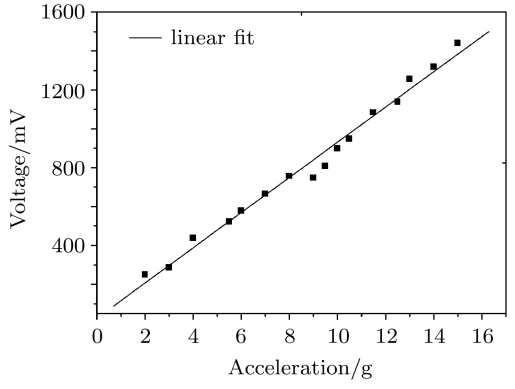


Fig.9. Voltages versus accelerations (within NDR region).

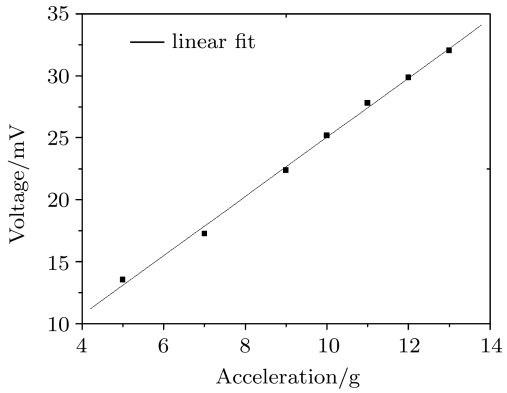


Fig.10. Voltages versus accelerations (beyond NDR region).

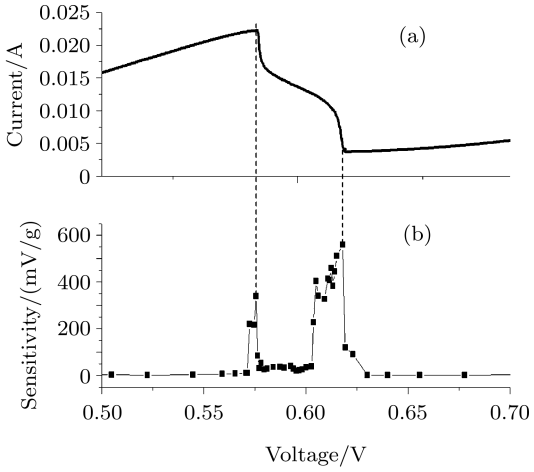


Fig.11. (a) I–V curve of RTD. (b) Sensitivity versus bias voltage of RTD.

4. Discussion

From Fig.11, it is known that the sensitivities within the NDR region are much higher than those beyond the region. At the bias voltage of 0.618 V, there is the largest sensitivity of 560.2025 mV/g, which is two orders higher than the smallest one 1.49135 mV/g at 0.755 V, therefore, the sensitivity of the accelerometer is adjustable in a range of 3 orders with the changing values of the bias voltage.

In order to compare the performance of the RTD based accelerometer with that of a silicon based one, a beam-mass structure of N-type silicon is designed, the

dimensions of the structure are the same with those of the fabricated accelerometer. In the structure, four P-type piezoresistors are diffused at the base of each beam to replace the RTDs. By utilizing finite element analysis method, the stress distribution of the structure is analysed. Subsequently, the longitudinal and transverse stresses along the pass at the base of the beam are 3.23 MPa and 0.683 MPa, respectively. For P-type piezoresistors, there is

$$\frac{\Delta R}{R} = \pi_{\mathrm{l}}\sigma_{\mathrm{l}} + \pi_{\mathrm{t}}\sigma_{\mathrm{t}} = (71.8S_x - 66.3S_y) \times 10^{-5},$$

where $R_0 = 50\Omega$ (according to Fig.8.), then the sensitivity is calculated to be about 50 mV/g. Comparing it with the values in Fig.11, we can know that the largest sensitivity of the RTD based accelerometer is about 10 times larger than that of the silicon based accelerometer.

5. Conclusion

An RTD based micro-accelerometer is designed and fabricated, an RTD-Wheatstone bridge based measurement system is established to detect the performance of the sensor. According to the experimental results, the sensitivity of the RTD based accelerometer is adjustable in a range of 3 orders by changing the bias voltage. The largest sensitivity of the accelerometer is 560.2025 mV/g, which is about 10 times larger than that of silicon based accelerometer.

References

[1] Chang L L, Esaki L and Tsu R 1974 *Appl. Phys. Lett.* **24** 593

[2] Yu R Y, Konishi Y, Allen S T, Reddy M and Rodwell MJW 1994 *IEEE Microwave Guided Wave Lett.* **4** 220

[3] Brown E R, Söderström J R, Parker C D, Mahoney L J, Molvar K M and McGill T C 1991 *Appl. Phys. Lett.* **58** 2291

[4] Chen C L, Mathews R H, Mahoney L J, Calawa S D, Sage J P, Molvar K M, Parker C D, Maki P A and Sollner TCLG 2000 *Solid-State Electronics* **44** 1853

[5] Guo T H, Lin H C, Potter R C and Shupe D 1991 *IEEE J. Solid State Circuits* **26** 145

[6] Hsin Hun Tung and Chien Ping Lee 1996 *IEEE J. Quantum Electronics* **32** 507

[7] Masahiro, Tsuchiya and Hiroyuki Sakaki 1986 *Appl. Phys. Lett.* **48** 88

[8] Sollner T C L G, Goodhue W D, Tannenwald P E, Parker C D and Peck D D 1983 *Appl. Phys. Lett.* **43** 588

[9] Guo W L, Niu P J, Liang H L and Zhang S L 2001 *6th Int. Conf. Solid State and Integrated Circ. Technol. Proc.* **2** 1403

[10] Mazumder P, Kulkarni S, Bhattachara M, Sun J P and Haddad G I 1998 *Proc. IEEE* **86** 664

[11] Williamson W (III), Enquist S B, Chow D H, Dunlap H L, Subramaniam S, Lei P, Bernstein G H and Gilbert B K 1997 *IEEE J. Solid-State Circuits* **32** 222

[12] Brugger H, Meiners U, Diniz R, Suski T, Gornik E, Foerster A and Luth H *Solid-State Electronics* **37** 801

[13] Fobelets K, Vounckx R and Borghs G 1994 *J. Micromech. Microeng.* **4** 123

[14] Mao H Y, Xiong J J, Zhang W D and Xue C Y 2006 *Chin. J. Semicond.* **27** 112 (in Chinese)

[15] Pritchard R, Klipstein P C, Couch N R, Kerr T M, Roberts J S, Mistry P, Soylu B and Stobbs W M 1989 *Semicond. Sci. Technol.* **4** 754

[16] klipstein P C 1995 *J. Phys. Chem. Solids.* **56** 435

[17] Wang J, Zhang W D, Xue C Y, Xiong J J, Liu J and Xie B 2007 *Chin. Phys.* **16** 1150

[18] Mutamba Kabula, Flath Michael and Sigurdardóttir Anna 1999 *IEEE Trans. Instru. and Measu.* **48** 1333

[19] Mutamba K, Sigurdardottir A, Vogt A, Hartnagel H L and Li E H 1998 *Appl. Phys. Lett.* **72** 1629

[20] Wen T D and Zhang W D 2003 *Micronanoelectronic Technology* **7/8** 41 (in Chinese)

[21] Xue C Y, Zhang W D, Xiong J J and Wen T D 2004 *International Workshop on Microfactories* **1** 498